2008

Anatomy and growth of a Holocene clinothem in the Gulf of Papua

Rudy Slingerland
The Pennsylvania State University

Neal W. Driscoll
Scripps Institution of Oceanography

John D. Milliman
Virginia Institute of Marine Science

Scott R. Miller
The Pennsylvania State University

Elizabeth A. Johnstone
Scripps Institution of Oceanography

Anatomy and growth of a Holocene clinothem in the Gulf of Papua

Rudy Slingerland,[1] Neal W. Driscoll,[2] John D. Milliman,[3] Scott R. Miller,[1] and Elizabeth A. Johnstone[2]

Received 6 July 2006; revised 15 April 2007; accepted 8 August 2007; published 5 March 2008.

[1] High-resolution seismic profiles and sedimentological data from grab samples and long cores provide an unprecedented picture of the structure, sedimentology, and late Quaternary development of two Gulf of Papua (GoP) clinothems, one probably Stage 3 and 4 in age and one Holocene in age. The older was partially eroded during Stage 2 and partially covered by the younger clinothem during Stage 1. The younger clinothem consists of three stratigraphic units separated by two surfaces of erosion, bypass, or correlative surfaces of lap. The surfaces were formed by changes in accommodation and sediment supply. The underlying physiography of the older clinothem also appears to play an important role in governing the shape of the younger clinothem. In the northern gulf, oblique clinoforms of the younger clinothem suggest that the rate of sediment supply from the northern rivers outstripped the formation of new accommodation, whereas in the south, sigmoidal clinoforms indicate that accommodation increased faster than sediment supply. The origin of the new accommodation remains uncertain because of limited age constraints. On the basis of sediment thickness, stratal geometry, and acoustic character, off-shelf transport appears to be the dominant sediment transport direction, with preferential accumulation on the promontories and bypass in the valleys. Presently, observed and computed modern flows and complex gyres in shallow water coupled with wave- and current-supported gravity flows or river floods can explain the form, internal clinoform shapes, and mineralogy of the younger Gulf of Papua clinothem.

Citation: Slingerland, R., N. W. Driscoll, J. D. Milliman, S. R. Miller, and E. A. Johnstone (2008), Anatomy and growth of a Holocene clinothem in the Gulf of Papua, *J. Geophys. Res.*, *113*, F01S13, doi:10.1029/2006JF000628.

1. Introduction

[2] Clinothems are the basic building blocks of modern and ancient continental shelves. Seismic and outcrop studies show that at least one-third of modern and ancient shelves have been built by the lateral stacking of such sedimentary packages [*Mitchum et al.*, 1977; *Kuehl et al.*, 1989; *Bartek et al.*, 1991; *Christie-Blick and Driscoll*, 1995; *Nittrouer et al.*, 1995; *Pirmez et al.*, 1998; *Driscoll and Karner*, 1999; *McCormick et al.*, 2000; *Hampson and Storms*, 2003; *Lofi et al.*, 2003; *Deibert et al.*, 2003; *Olariu and Bhattacharya*, 2006; *Cattaneo et al.*, 2004; *Liu et al.*, 2004b]. The lateral stacking patterns exhibit a variety of geometries such as sigmoid, oblique, and parallel (as first classified by *Mitchum et al.* [1977]), but all have in common a lateral translation of a relatively self-similar form. Here we use the term *clinoform* for the chronostratigraphic horizon cutting obliquely through a heterolithic, coarsening upward sequence (as per *Mitchum et al.* [1977]), such as imaged by a single seismic reflector, and the term *clinothem* to indicate a deposit containing such surfaces. We also separate clinothems into two types: those with subaerial topsets (deltas and shorefaces) and those without (subaqueous clinothems).

[3] Subaqueous clinothems, and their evolution through time as reflected in their clinoforms, are thought to be a function of four semi-independent variables: rate of creation of accommodation, type and mass of sediment flux to the shelf, the processes distributing that sediment across the shelf, and stage of development (Figure 1). If we knew the functional relationship between the dependent variables (geometry, facies, and evolution of clinothems), and the independent variables, we could predict better the long-term fate of shelf sediment and hindcast the history of relative sea level, sediment flux, and shelf processes as recorded by clinoforms. Developing this functional relationship has proceeded along the traditional lines of theory (see *Driscoll and Karner* [1999] and *Kostic and Parker* [2003a, 2003b] for reviews), experiment [*Paola et al.*, 2001; *Pratson et al.*, 2004; *Niedoroda et al.*, 2005], and observation.

[4] Observational studies conducted on many modern clinothems around the world provide specific realizations of the functional relationship between clinothem characteristics and the controlling independent variables. The Amazon was the first to be well studied and remains the archetype subaqueous sigmoidal clinothem [*Kuehl et al.*, 1986; *Nittrouer et al.*, 1986; *Nittrouer et al.*, 1995]. Rollover occurs in 40 m water depth over 150 km from the

[1]Department of Geosciences, Pennsylvania State University, University Park, Pennsylvania, USA.
[2]Scripps Institution of Oceanography, La Jolla, California, USA.
[3]School of Marine Science, College of William and Mary, Gloucester Point, Virginia, USA.

0148-0227/08/2006JF000628

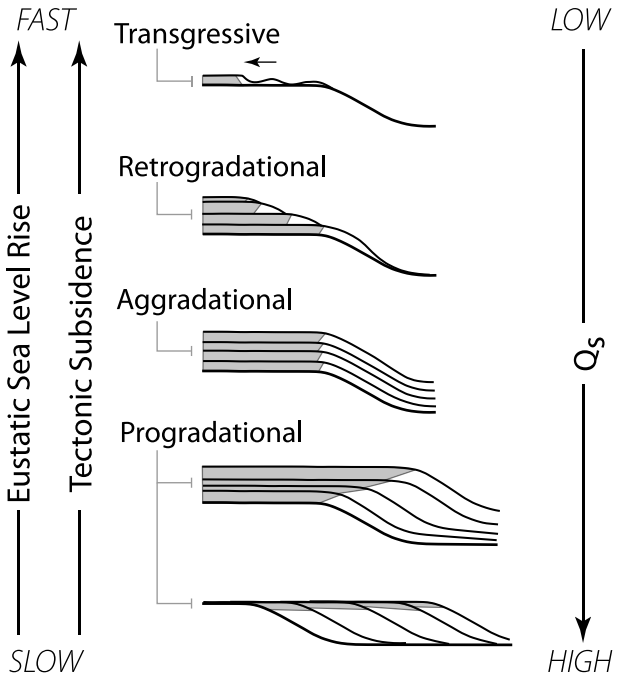

Figure 1. Schematic illustrating the interplay between sediment supply and accommodation in controlling clinoform geometry. Accommodation records both changes in eustatic sea level and tectonic subsidence/uplift. When sediment supply (Q_s) is greater than new accommodation, progradation occurs. Oblique progradation is a special case where no new accommodation is created. Aggradation occurs when sediment supply is equal to accommodation, while backstepping (retrogradational) results when sediment supply is less than accommodation.

coast. Foresets extend to 60 m water depth, dipping relatively steeply (but still less than 1°). *Kuehl et al.* [1986] proposed that sediment-laden buoyant plumes are the delivery mechanism for clinothem growth. Subsequent AmaSeds work [*Kuehl et al.*, 1996; *Nittrouer and DeMaster*, 1996; *Nittrouer et al.*, 1996] showed that the surface low-salinity plume is decoupled from clinoform development and *Kineke et al.* [1996] outlined the importance of hyperpycnal processes on its development.

[5] Quaternary shelves of the Mediterranean show a range of clinothem types from parallel delta/shore clinothems in the Gulf of Lions [*Berne et al.*, 2004] to sigmoidal subaqueous on the Italian Adriatic shelf [*Cattaneo et al.*, 2004]. The late Holocene clinothems are all fine-grained, about 35 m thick with the rollover in about 25 m water depth, and contain clinoform surfaces that dip at less than 1°. Because they extend downdrift for hundreds of kilometers from their parent deltas, it is clear that sediment transport by wind-driven coastal currents with bottom Ekman transport plays a large role in their growth. These geometrical characteristics are remarkably similar to both the Holocene Yellow and Yangtze River clinothems that extend downdrift for hundreds of kilometers along the China coast [*Hori et al.*, 2002b; *Chen et al.*, 2003; *Liu et al.*, 2004a, 2004b].

[6] The Ganges-Brahmaputra subaqueous clinothem rolls over in about 30 m water depth and in most other attributes is similar to the Amazon and Yellow River clinothems [*Kuehl et al.*, 1989, 2005; *Michels et al.*, 1998]. Fine-grained muddy beds of the foreset are thought by *Michels et al.* [1998] to be formed by "slowly moving suspension-rich plumes" (p. 147), decimeter and thicker graded, sand and silt layers by cyclone-generated coastal currents, and acoustically transparent layers by mudflows. It is an interesting point that most modern subaqueous clinothems are built by oblique, along-shelf transport [*Driscoll and Karner*, 1999], even though most conceptual models to date ignore the along-shelf dimension.

[7] These modern studies are supplemented by numerous observations of ancient clinothems. The relationships between form and process can only be broadly inferred, but the geometries provide a useful addition to the database. According to *Steckler et al.* [1999], Miocene subaqueous clinothems of the New Jersey margin were initiated because of increased sediment supply. As they prograded into deeper water they increased in steepness and height, ranging from less than 100 to 700 m [*Poulsen et al.*, 1998]. Other examples include storm-wave-dominated Eocene clinoforms of Spitsbergen [*Deibert et al.*, 2003], reaching heights of 150 m and foreset dips of 4°; and Cretaceous sandy shoreface clinoforms from Utah with heights averaging 20 m and foreset dips less than 1° [*Hampson and Storms*, 2003].

[8] The purpose of this work is to contribute to the growing observational database upon which a definition of the functional relationship between form and process will ultimately depend. Here we present the surface morphology and internal stratigraphy of a modern subaqueous clinothem in the Gulf of Papua on the southeastern coast of Papua New Guinea as imaged by 2-D chirp survey and piston cores. Our observations show that this clinothem is a composite feature built by oblique alongshore stacking of sediment packages as sediment from multiple sources is transported along as well as across-shore, in contradistinction to the standard two-dimensional model of relatively uniform along-strike growth seaward.

2. Study Area

[9] The study area lies on the central shelf of the Gulf of Papua (GoP) (Figure 2), a semicircular embayment off the northern Coral Sea. It is underlain by shelf sediments at depths from 0 to 120 m (mean depth = 50 m) and bordered to the north and west by the mangrove shoreline of Papua New Guinea. It is fed freshwater and sediment by five principal rivers—the Fly, Bamu, Turama, Kikori, and Purari (Table 1 and Figure 2). Their estimated collective freshwater discharge is about 15,000 $m^3\ s^{-1}$ [*Wolanski et al.*, 1995], more or less evenly distributed both seasonally and interannually such that the 100-year floods of the Fly and Purari are only about twice the size of the 2-year floods [*Pickup*, 1984]. Collectively these rivers deliver somewhere around 200 million tons a^{-1} to their respective floodplains, deltas, and the gulf (J. Milliman, unpublished data, 1999). Although the Fly contains by far the largest water discharge, its sediment load is relatively modest because the source rock lithology is limestone-dominated [*Brunskill*, 2004] (Table 1), and the large floodplain still contains unfilled accommodation because of the post-LGM rise in sea level. Approximately 90 percent of the Fly sediment

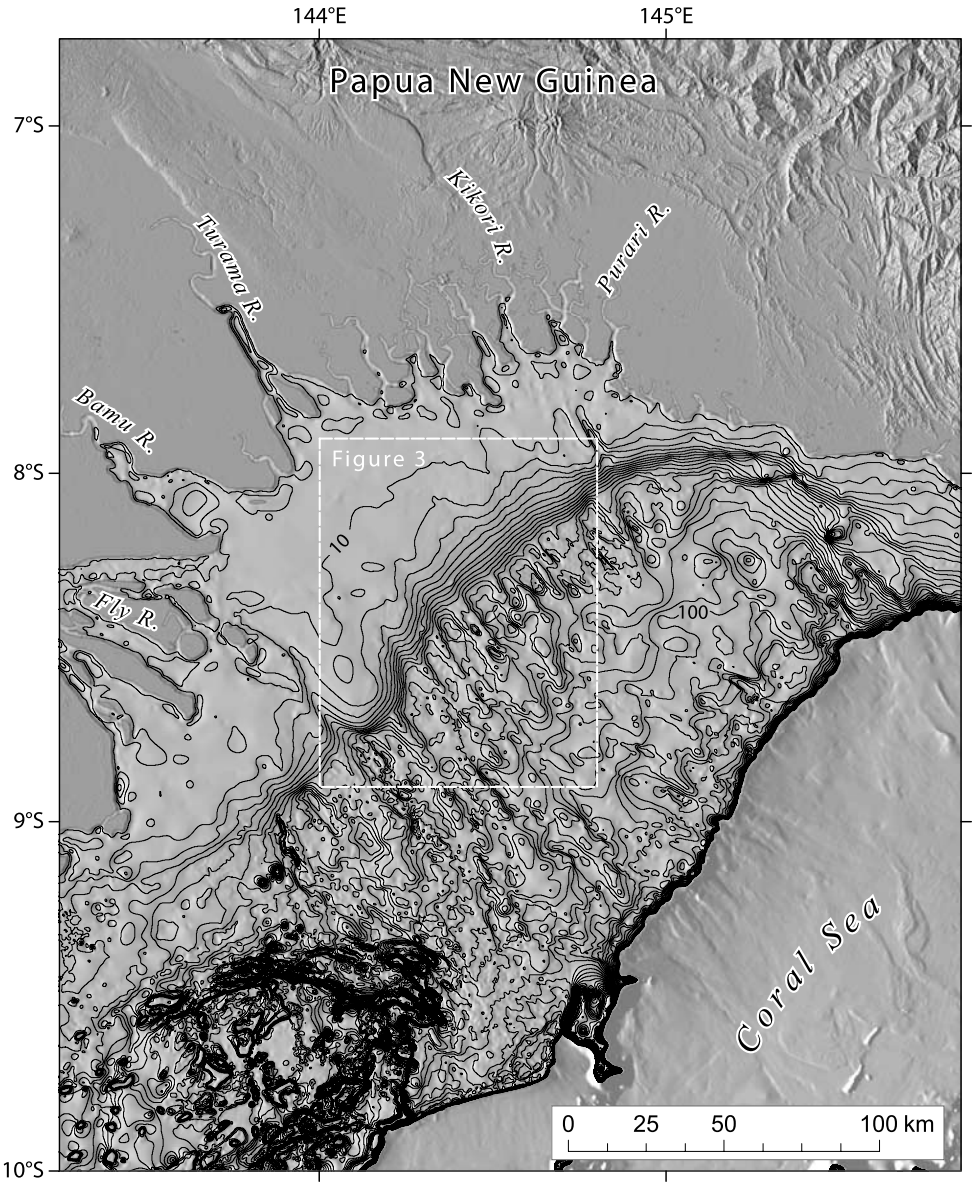

Figure 2. Location of study area (box) showing Gulf of Papua. Bathymetry of shelf in 5 m intervals from 5 to 200 m below sea level (digital data from *Daniell* [2008]). Bathymetry shaded from west.

delivered to the coast is finer than sand size [*Wolanski and Alongi*, 1995]; the sediment is relatively mature with high quartz/feldspar and illite/smectite ratios. The steep northern rivers in contrast, have much higher sediment yields and the sediment is an immature mix of volcaniclastic and other lithic fragments, thereby providing a convenient tracer for sediment transport on the GoP shelf [*Milliman*, 1995; *Brunskill*, 2004]. No estimates of size grading for the northern rivers are available, but the floodplains are narrow and short, suggesting that a greater percentage of sand can be expected to reach the coast.

[10] Sediment delivered to the shelf is thought to be distributed by a combination of tidal, wind-driven, oceanic, and thermohaline currents [*Harris*, 1990; *Wolanski and Alongi*, 1995; *Harris et al.*, 1996; *Walsh et al.*, 2004; *Keen et al.*, 2006; *Ogston et al.*, 2008; *Slingerland et al.*, 2008]. Tides on the shelf in 70 m water depth away from river mouths are mostly semidiurnal [*Wolanski et al.*, 1995; *Ogston et al.*, 2003; *Harris et al.*, 2004; *Ogston et al.*, 2004] and cross-shore. Most of the shelf is mesotidal. Wind-driven currents show two dominant circulation states highly influenced by seasonal monsoon/trade winds [*Wolanski et al.*, 1995; *Hemer et al.*, 2004; *Keen et al.*, 2006; *Slingerland et al.*, 2008]. During the northwest monsoon (December to March) flows on the topset are dominated by tidal variations and river discharge. Net (tidally averaged) flows are generally weak ($\sim$0.01 m s^{-1}) and offshore at the surface, with periods of southerly flow. Flows at the bed are also primarily tidal in nature, and are generally equal in magnitude to flows at the surface, but onshore. Flows over the clinoform face retain a strong tidal signature; however, like the flows on the topset, the net surface flow is weakly ($\sim$0.03 m s^{-1}) offshore. At the toe of the clinothem the SW-directed bottom flows of the outer shelf deflect to the NW as

Table 1. Characteristics of Rivers Draining Into the Gulf of Papua

	Fly	Bamu	Turama	Kikori	Purari	Total
Drainage basin area[a], km^2	62,728	7128	4528	19,800	29,588	123,782
Water discharge[b], $m^3\ s^{-1}$, 1986	6000[c]	2000	2000	2000	3000	15,000
Sediment discharge[d], 10^6 tons a^{-1} [*Wolanski et al.*, 1995]	80	low	low	50	60–70	200–365
Percent carbonate in catchment [*Milliman*, 1995; *Milliman et al.*, 1999]	70	?	?	60	20	
Percent volcaniclastic in catchment [*Brunskill*, 2004]	<5	?	?	30	35	

[a]Estimated by basin analysis of the ETOPO5 DEM.
[b]These values are estimates mainly from *Wolanski et al.* [1984], who provide some data for 1979 for the Kikori River (eight complete months and four part months) and for the Purari River (six part months). Additional data for the Fly are from *Salomons and Eagle* [1990].
[c]Of this amount, 60–80% exits by the southernmost distributary [*Harris et al.*, 2004].
[d]Range reflects uncertainties and estimates by various researchers. Values of individual rivers do not sum to estimated total because estimates for individual rivers are based on the drainage area method of *Harris et al.* [2004].

they climb the face, while maintaining their intensity (0.01 m s^{-1}). These climbing flows are the source of the upwelling observed on the clinothem topset. The trade wind season (May to November) is marked by surface and bottom flows on the topset that are roughly equal in magnitude to their monsoon counterparts (~0.02 m s^{-1}), but primarily directed NE. Flows over the clinoform face are parallel to the bathymetric contours and directed NE. These results suggest a sediment dispersal pattern on the modern clinothem topset of offshore surface transport with both SW and NE alongshore components, dependent upon the season. Upwelling on the clinoform face acts to localize deposition there and keep the outer shelf relatively sediment starved [*Moore and MacFarlane*, 1984; *Wolanski and Alongi*, 1995; *Wolanski et al.*, 1995; *Slingerland et al.*, 2008].

[11] Previous work on the GoP clinothem [*Harris et al.*, 1996; *Walsh et al.*, 2004] has demonstrated that discrete, yearly depositional events appear to be the fundamental building unit of the GoP midshelf modern clinothem. According to *Walsh et al.* [2004], the clinoform face is created by fluid mud deposition in response to the transition from trade to monsoon wind conditions, although precisely how this happens in the presence of onshore bottom flows is as yet unknown. Detailed ^{210}Pb and grain-size data indicate that low activities and increased clay contents are associated with discrete decimeter-thick layers that preferentially accumulate on the foresets of the clinothem. Short-term (based primarily on ^{210}Pb) rates of deposition are as high as ~4 cm a^{-1} [*Walsh et al.*, 2004]. Here we extend these observations to the millennial and longer timescales.

3. Methods

3.1. Chirp Data

[12] As part of the NSF MARGINS initiative, more than 6800 km of high-resolution chirp seismic data (2300 km of surface-towed Edgetech and 4500 km of hull-mounted Knudsen) were acquired between September 2003 and March 2004 aboard the RV Melville (cruises VANC22MV and VANC23MV; see http://www.marine-geo.org/margins/ for cruise information). Here we focus on the central portion of the GoP clinothem (Figure 3) over which 670 km of seismic data were collected with penetration 50–100 m below the seafloor. These high-frequency seismic data permit submeter geologic resolution. Basic sequence stratigraphic methods for identifying and interpreting surfaces were employed [e.g., *Christie-Blick and Driscoll*, 1995]. Seismic lines were interpreted on paper and in Seisworks 2D by identifying terminations and then using horizons of terminations to define surfaces. Termination types include onlap, downlap, truncations, and toplap. Surface types include unconformities (local and regional), surfaces of progradation (downlap), retrogradation (onlap), and accretion (onlap and downlap).

[13] Two-way times (TWTs) to the seafloor and various surfaces were converted to depths assuming a seismic velocity in sediment of 1750 m s^{-1}, a value typical of uncompacted nearshore sediment. The depth difference between the seafloor and a surface yields the thickness of sediment above the surface. The thicknesses were interpolated with an inverse distance weighted method to create an isopach map. For this interpolation, data were resampled at a coarser resolution (one data point every 500 seismic traces rather than one data point per trace) and the closest 50 points were used in the calculation. TWTs to the seafloor varied

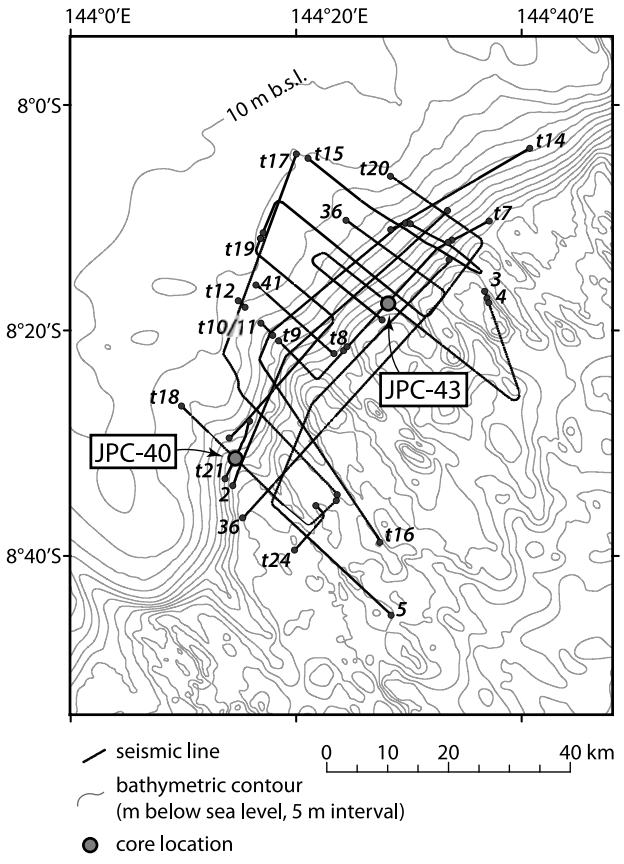

Figure 3. Bathymetric map of the central lobe showing chirp lines used in this study.

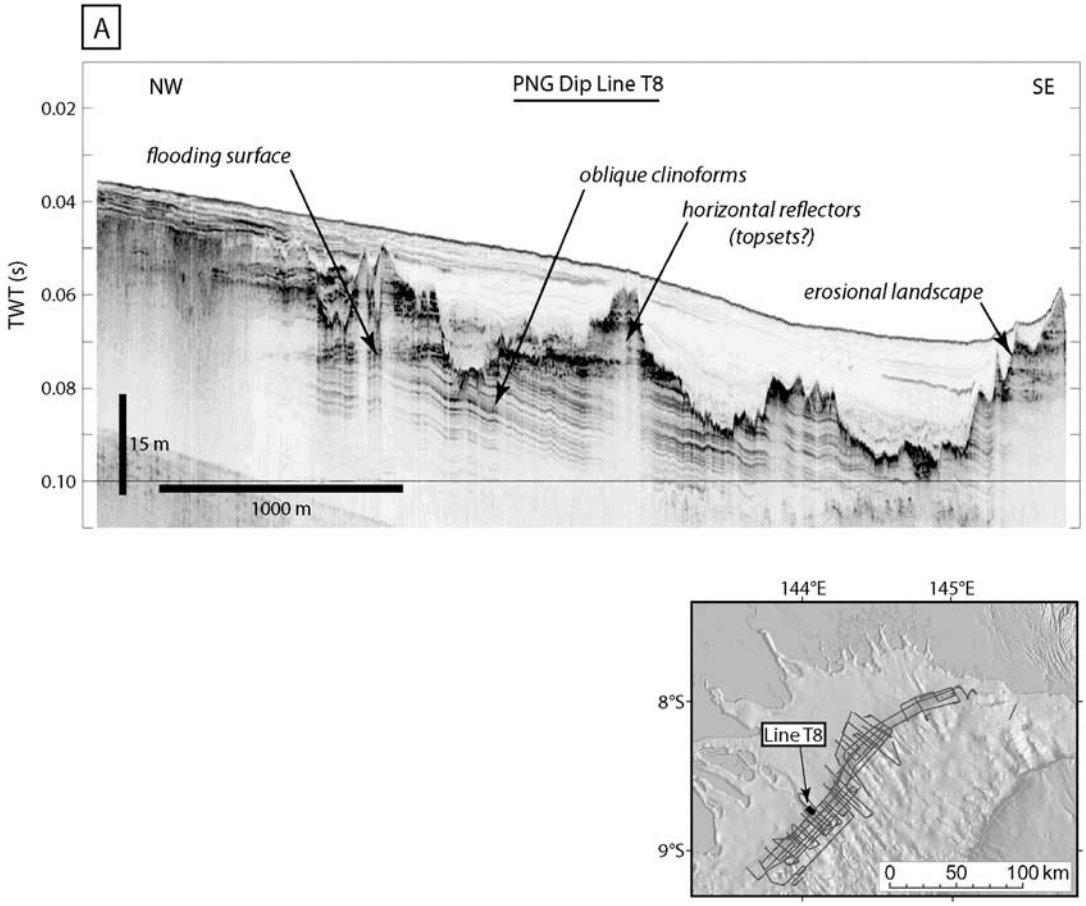

Figure 4a. Chirp subbottom profile Papua New Guinea (PNG) Dipline T8 shows an older clinothem consisting of oblique clinoforms mantled by flat-lying strata above a flooding surface. Above a significant erosional unconformity lies the modern clinothem, here represented by seaward dipping reflectors.

among lines and within lines because the chirp system is deep-towed. Without an independent constraint on the actual seafloor TWT or depth, the TWT or depth to any horizon is not very meaningful. Therefore to create a structure map of a surface, the isopach grid was subtracted from a grid of bathymetry. Reflector dips were determined by measuring apparent dips in two intersecting seismic lines, then solving for true dip as a three-point problem.

3.2. Core Data

[14] Ten piston cores and 7 gravity cores were taken in the study area, and from these, cores JPC-40 (8° 31.4041′ S; 144° 14.7091′ E) and JPC-43 (18° 17.0302′ S; 144° 27.4946′ E) were chosen for radiocarbon dating at the National Ocean Sciences Atomic Mass Spectrometer facility at the Woods Hole Oceanographic Institution, USA, yielding six dates. Figure 3 gives the core locations with respect to the chirp lines.

4. Observations

4.1. General Morphology and Stratigraphy

[15] As first pointed out by *Harris et al.* [1996], the morphology of the GoP shelf consists of two treads separated by a riser (Figure 2). The upper tread is the smooth and gently seaward sloping seabed extending up to 60 km from a mangrove-fringed shoreline to water depths of 20 m where dips increase to 0.2 to 0.8° on the riser. From the toe of the riser in water approximately 80 m deep, the lower tread is the seabed extending seaward 100 km to the shelf edge at 120 m water depth. Unlike the smooth upper tread and riser, the lower tread is corrugated with a NW–SE-trending lineation.

[16] The treads and risers are created by two stacked clinothems—an older deeply eroded clinothem forming the middle (and possibly outer) shelf, and a superjacent younger clinothem extending from the coast offshore forming the inner shelf (Figures 4a–4d). The older, eroded clinothem consists of approximately 30–40 m of generally subhorizontal reflectors lying beneath an erosional surface with marked truncation (Figure 4a). The subhorizontal, concordant reflectors exhibit minimal thickness variations (Figure 4b) and cap a set of obliquely prograding reflectors (Figure 4c) that extend tens of kilometers across the margin. The change in geometry (i.e., oblique progradation to aggradation) allows us to infer the relationship between sediment supply and accommodation (e.g., Figure 1). The oblique clinoforms can be traced across large portions of the GoP shelf and indicate that sediment supply was infilling the available accommodation. The geometry of the overlying aggrading parallel concordant sequence indicates that the creation rate of new accommodation was equal to the rate of sediment supply. In the central gulf

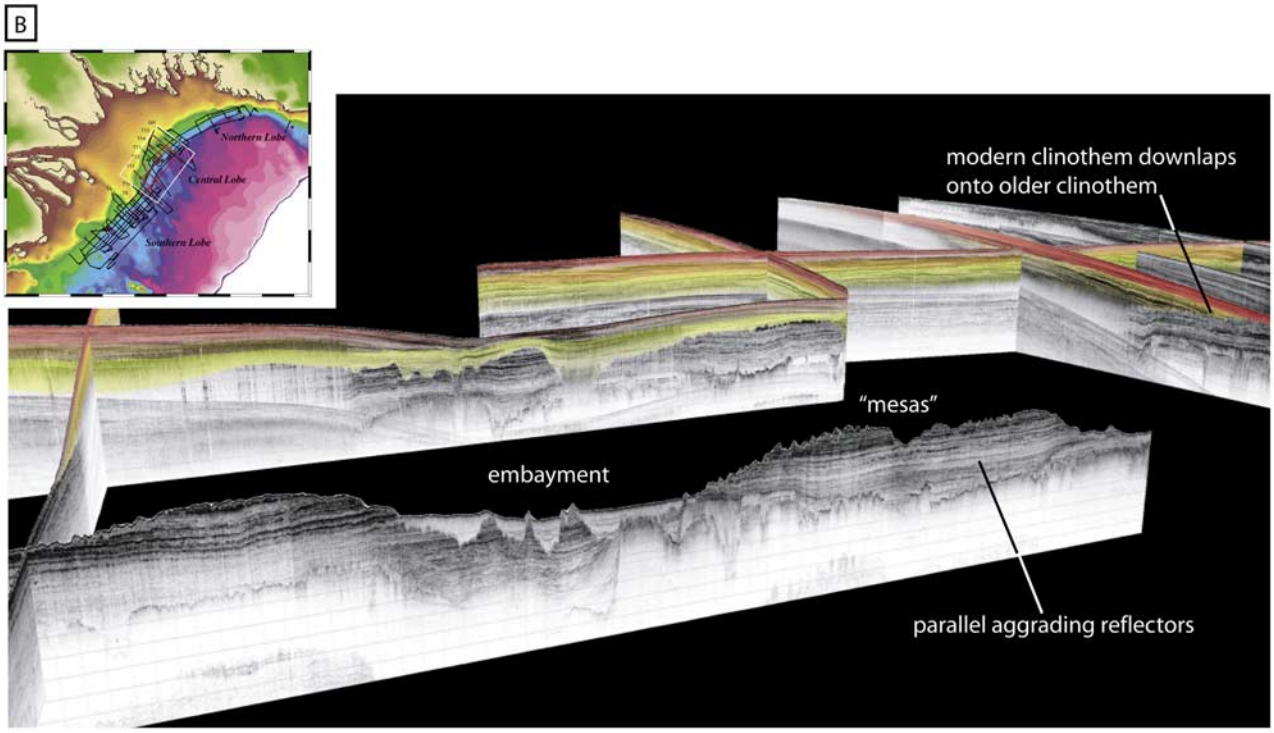

Figure 4b. Chirp fence diagram looking NW along the central lobe on the GoP shelf illustrates the parallel, concordant sequence of the older clinoform. Individual horizons within this sequence can be traced laterally along the margin for great distances with minimal thickness variations. Several valleys or embayments dissect the margin, and intervening highs or erosional "mesas" exhibit marked truncation along their borders. Offshore on the middle and lower tread this erosional morphology outcrops on the seafloor and is only partially infilled in the embayments, which gives rise to the rough corrugated morphology observed in the bathymetry. Landward, the modern clinoform obscures the underlying erosional landscape. Inset shows location of fence diagram.

midshelf region, northeast of the Fly River mouth, this older clinothem has been dissected by six major valleys ranging in width from 10 to 15 km, cut into the subhorizontal strata and separated from one another by "mesas" [*Harris et al.*, 1996] that stand 10–20 m higher than the valleys (Figure 4b). Cut into both the valleys and mesas are numerous channels, mostly less than ~200 m wide but as much as 30–40 m deep (Figure 4d).

[17] The younger clinothem downlaps onto the erosional surface etched into topsets of the older clinothem (Figures 4 and 5). Its face undulates along strike in a series of subtle promontories and reentrants (Figure 2) that correlate with the mesas and paleovalleys etched into the underlying older midshelf clinothem. This erosional landscape creates a variation in accommodation that shapes the overlying sequence. The modern clinoform exhibits both onlap and downlap patterns and these wedges near the base of the clinoform tend to diminish the observed relief. It appears that theses onlapping wedges in Line PNG00-03 (Figure 4c) are recording oblique along-shelf transport. The importance of along-shelf versus across-shelf transport in clinoform development needs to be understood and quantified.

4.2. Description of Stratigraphic Units in the Younger Clinothem

[18] The younger clinothem in the study area consists of three major stratigraphic units (here called Yellow, Orange, and Red) that are separated by two surfaces of erosion or correlative surfaces of down/up/on/off-lap (Figures 5, 6, and 7). The most prominent surface (surface S_1) separates Yellow from the Orange and Red units everywhere in the study area. To the NE it is an erosional unconformity or surface of bypass (e.g., Figure 5); to the SW it is a surface of lap. Below S_1 lies the oldest unit imaged (Yellow in Figure 6), which is present everywhere in the study area. It is acoustically well bedded, prograding (Figure 7), and in places folded, possibly due to soft sediment deformation (Figures 6 and 7).

[19] Above the S_1 surface lie the Orange and Red units. The Orange unit is the older of the two and only occurs in the southern portion of the study area. It is a convex upward body built by accretion beds prograding obliquely both ENE and S. It is acoustically bright and well-bedded. The Red unit drapes both the Orange and Yellow units above a surface of lap (S_2) and is present everywhere in the study area. It is more acoustically transparent and built by up- and down-lapping beds (Figures 6 and 7). Grab samples and cores show that the Red and Orange units consist of three principal facies. By far the most voluminous is Facies 1, a dark gray homogeneous, very fine silty clay (cf. Figures 8 and 9) with occasional well-laminated intervals. Facies 2 consists of very thin interbeds of dark brown very fine sand. Based mostly on correlation with cores taken outside the central study area, Facies 3 consists of muddy fine to very fine sand; superficial iron-stained magnesian-calcitic ooids characterize this facies.

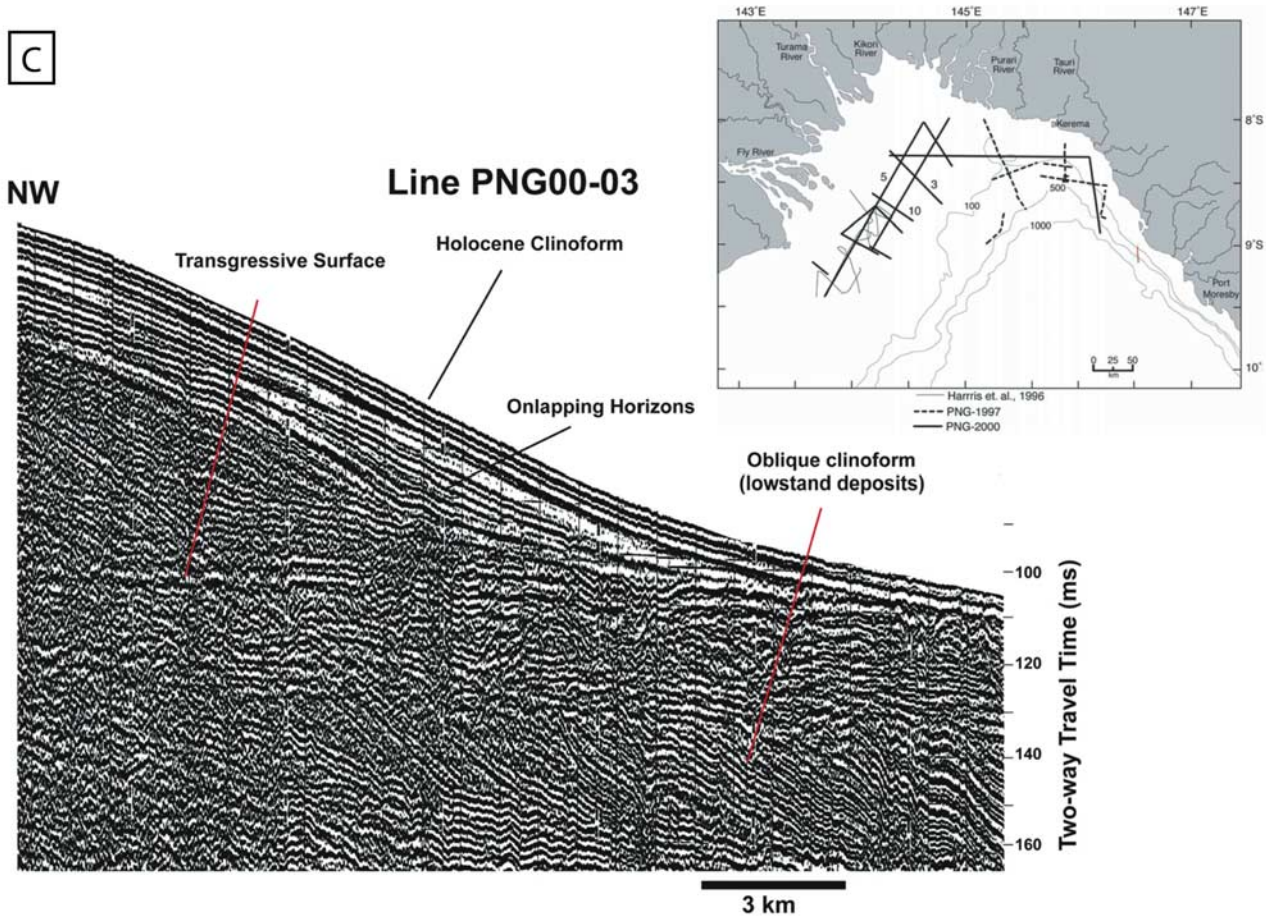

Figure 4c. Sparker profile PNG00-03 acquired in the GoP is roughly coincident with transect H [see *Aller et al.*, 2008] and images the older clinothem. Older clinothem comprises an oblique prograding package mantled by a parallel concordant package. Note that 10 ms is approximately equal to 7.5 m two-way travel time.

[20] The ages of the bounding surfaces are not well constrained. Of the 29 cores taken in the central study area, only one (JPC-40; Figure 8) may have penetrated the Yellow unit, but this core experienced significant flow-in upon extraction. Assuming that all the dated samples come from above S_1, we can say that the S_1 surface must be older than 5.21 ka BP. Core JPC-43 (Figure 9) penetrates 11 m of the Red unit to within 1.5 to 2 meters of S_1. Radiocarbon ages of bulk carbonate from 3, 4.5, and 7 m deep in the core are 1.75, 1.57, and 1.84 ka BP, respectively, yielding a youngest possible age for the S_1 surface of 1.84 ka BP. A core (JPC-02) taken at 7° 58.6841′S; 145° 2.9818′E provides some additional evidence that the S_1 surface is earliest Holocene. An ooid facies in JPC-02 ends abruptly at ~4 m, above which the sediment consists of silty clay. The ooids at 4 m have an age of ~9.5 ka BP, yielding sediment accumulation rates between 4 and 9 m depth in the core of about 2.5 mm a^{-1}. Above ~3.5 m, accumulation rates appear to be <1 mm a^{-1}.

[21] A structure map on the S_1 surface (Figure 10) shows its elevation with respect to sea level. On the whole the reentrants and promontories in the paleobathymetry and modern bathymetry are spatially correlated, indicating that the growth of the clinothem has been roughly self-similar over the last few thousand years. An isopach map created by contouring vertical distances between the structure contour map and the present seabed (Figure 11) shows that the thicknesses of sediment overlying S_1 range from 0 to 38 m. Three depocenters of maximum thickness lie along the upper face of the modern clinothem coincident with the bathymetric promontories. In contrast, on the lower face the depocenters of maximum thickness lie in bathymetric reentrants. Chirp strike lines crossing two promontories in the central region about midway down the clinothem face (Figure 12) show that variations in thickness of the Yellow unit smooth out the paleotopography.

[22] The Orange and Red units overlying S_1 exhibit an interesting constructional character, with the greatest thicknesses on the highs and systematic thinning toward the valleys. In addition, high-amplitude reflectors are preferentially observed within the valleys in the Orange and Red units. Even given these thickness differences, units above and below the S_1 surface show a similarity in reflector dips and dip directions (Figure 13) at a given site. Differences in attitudes are small in comparison to changes among sites, again indicating self-similar growth.

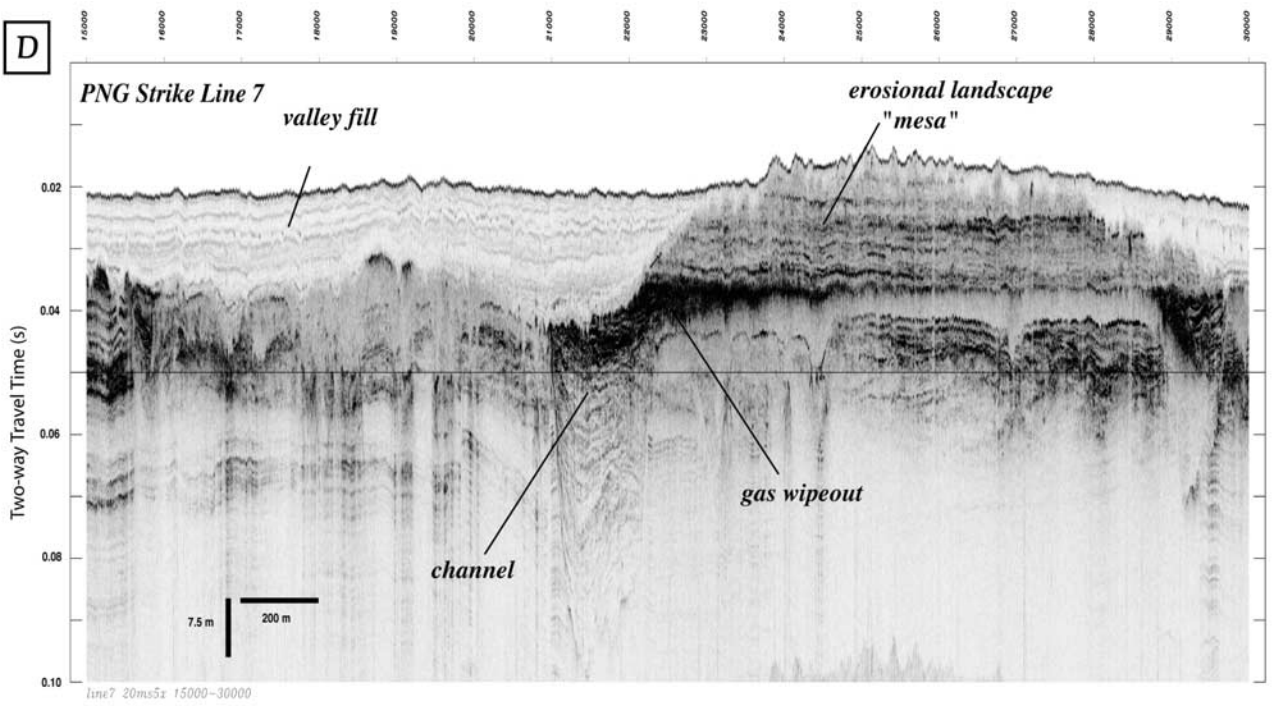

Figure 4d. Chirp profile Line 7 across an erosional mesa and adjacent valley or embayment illustrates the parallel nature of the concordant sequence of the older clinoform and shows erosional truncation and downcutting along the edges of the mesa. Close to the margin the valleys are preferentially filled, and the fill onlaps onto the erosional landscape. Within the valleys are incised channels that are approximately 200 m wide and up to 20–40 m deep.

4.3. Stratal Relations With Adjacent Portions of the Clinothem

[23] Reflectors in the study area are downlapped both to the north and south by younger reflectors (E. A. Johnstone et al., Clinoform architecture in the Gulf of Papua records the interplay between sea level, sediment supply, and climate, submitted to *Geology*, 2008; hereinafter referred to as Johnstone et al., submitted manuscript, 2008),

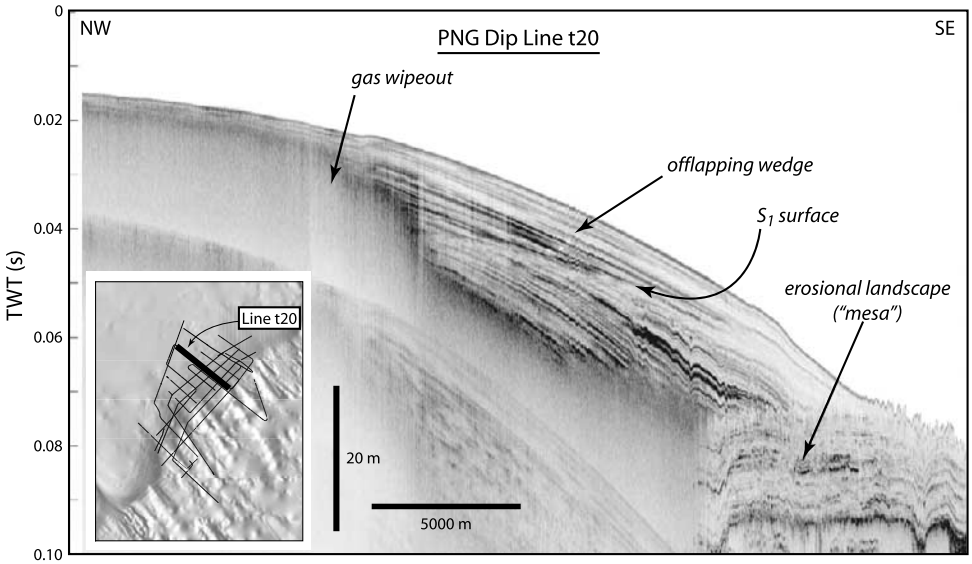

Figure 5. Chirp subbottom profile showing downlapping of younger clinoforms onto topsets of older clinothem (see Figure 2 for location). Surface of erosion or bypass is recorded by the S_1 horizon (see section 4.2 for details).

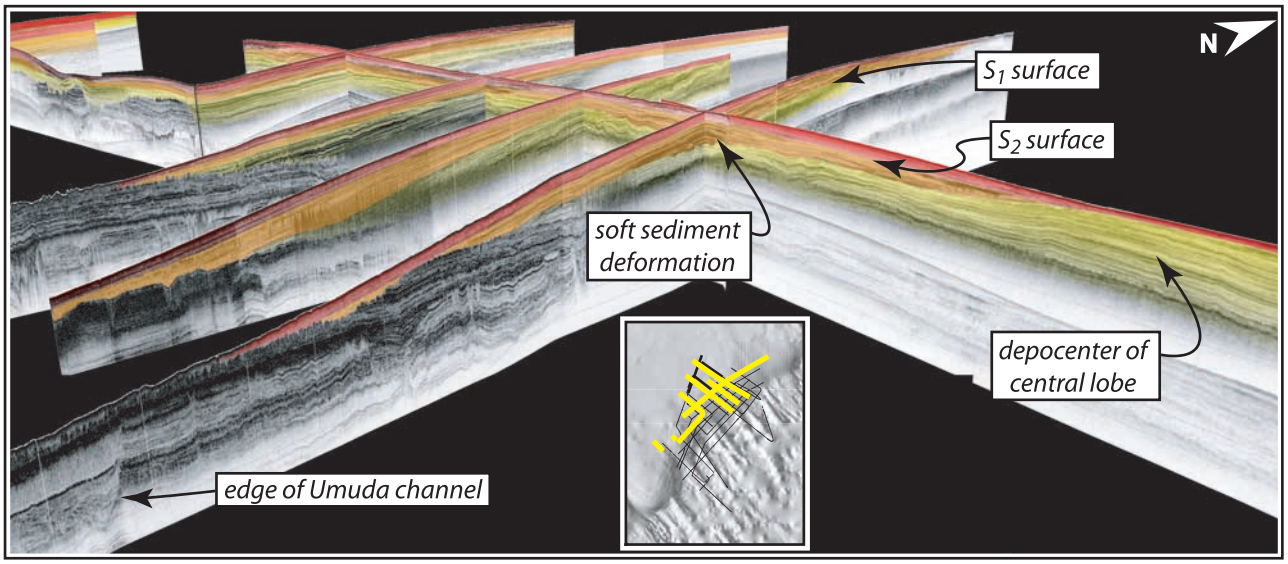

Figure 6. Seismic fence diagram of study area looking southwest along the Holocene clinoform face (see Figure 2 for location). Three stratal units are separated by two surfaces of erosion and lap. Lowest and most regionally extensive surface (S_1) separates an older, more acoustically laminated, obliquely prograding, and in places, folded unit (Yellow unit) from two younger units that are more acoustically transparent, unfolded, and up-building (Orange and Red). Surface S_2 separates a localized acoustically bright unit (Orange) from an acoustically transparent regional drape (Red). (See Johnstone et al., submitted manuscript, 2008, for a more detailed description).

indicating that the standard view of clinothems as two-dimensional prograding bodies is not applicable here. The polygenetic nature of this Holocene clinothem is also indicated by the mineralogy of its surficial sediments. Illite/smectite ratios in the clay fraction (Figure 14) and quartz/feldspar ratios in the 62–90 μm fraction (not shown) can be interpreted to reflect a mixing of subarkosic sands and illite-dominated muds delivered by the Fly River from the south with immature arkosic sands and smectite-dominated muds

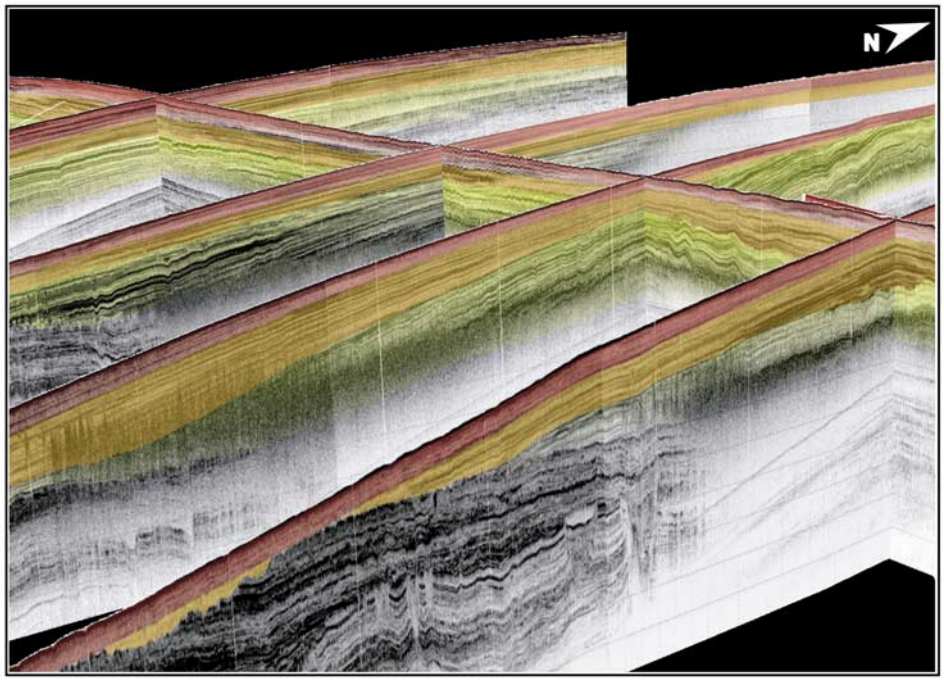

Figure 7. Enlargement of Figure 6 showing the transition from oblique progradation near depocenter to sigmoidal progradation on southern edge of the study area. Also note folds in Yellow unit.

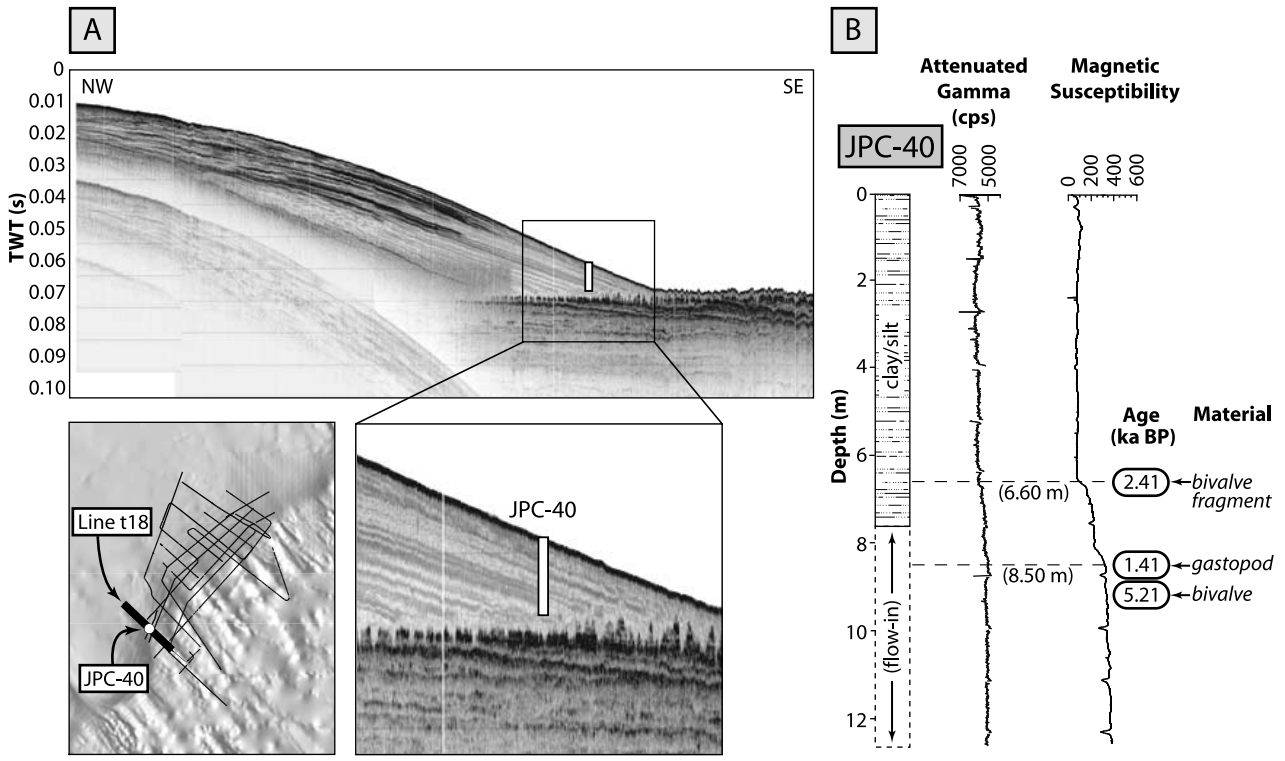

Figure 8. (a) Chirp Track 18 Line 4 showing location of JPC-40. (b) Core lithic log, attenuated gamma and magnetic susceptibility logs, and radiocarbon ages. Sediment below 670 cm in the core was sucked into the core barrel upon extraction, possibly explaining the mixture of radiocarbon ages. Red unit consists of very dark gray homogenous silty clay deposited over the last 5.21 ka.

delivered by the steeper rivers tapping the volcanogenic terrain to the north (Table 1).

5. Interpretation

5.1. Geologic History of the Gulf of Papua Shelf

[24] The upper approximately 100 m of the GoP shelf consists of two stacked clinothems: an older, partially eroded clinothem forming the floor of the middle shelf, and a Holocene clinothem forming the inner shelf. On the basis of the stratal geometry of the older clinothem and its present elevation, we deduce that it prograded two-thirds of the way across the preexisting shelf in response to a relative sea level fall during Stage 4 (Figure 15), when the rate of sediment supply filled the available accommodation. We infer that these oblique clinoforms were deposited during Stage 4 (~55,000–75,000 years BP) because we observe no aggradation during progradation (e.g., Figures 4a and 4c); this requires a rate of eustatic sea level fall that is faster than subsidence. This inference is consistent with a major siliciclastic pulse observed on the slope between 60,000–100,000 years BP [*Mallarino et al.*, 2004].

[25] Above the oblique clinoforms lie parallel reflectors that represent topsets (e.g., Figure 4). Using sequence stratigraphic principles we infer that these topsets formed when the rate of sediment supply equaled the creation of new accommodation (e.g., Figure 1) during Isotope Stage 3 prior to the large sea level fall associated with the LGM (Figure 15). This age is consistent with data from several cores acquired by *Harris et al.* [1996] which recovered Pleistocene sediments from the top of the parallel sequence where exposed at or near the seafloor. Core 37PC11 from the top of an erosional "mesa" yielded a radiocarbon date of 33,850 years BP [*Harris et al.*, 1996] and other cores from the "mesa" features that sampled the parallel, concordant unit (e.g., Fr-93–1PC1, 30PC8) recovered Pleistocene deltaic facies and cohesive reddish brown clays. On the basis of these observations, *Harris et al.* [1996] suggested that the pretransgressive deposits were deposited 50,000–20,000 years BP, consistent with our interpretation. If correct, such a scenario suggests that tectonic subsidence in the region was outpacing the slow eustatic fall during Stage 3 (~1 mm a^{-1}) to create the available accommodation (Figure 15).

[26] This magnitude of differential tectonic subsidence (~1 mm a^{-1} or 10 m/10,000 years) is problematic. Dated coral material acquired from fringing reefs along the Ashmore Trough at 125 m water depth (Core MV-73) suggests there has been little to no tectonic subsidence since the LGM in that region [*Droxler et al.*, 2006]. However, Core MV-73 was acquired south of the peripheral bulge for the GoP foreland basin (Figure 2) and thus might not reflect tectonic subsidence within the foreland. Furthermore, the tectonic subsidence rate demanded by the parallel, concordant topsets observed in the older clinoform is consistent with differential tectonic subsidence rates determined from exploratory wells in the region (e.g., Borabi-1 and Pasca C1; [*Davies et al.*, 1989]). In addition, the transgressive surface formed as a consequence of the rapid

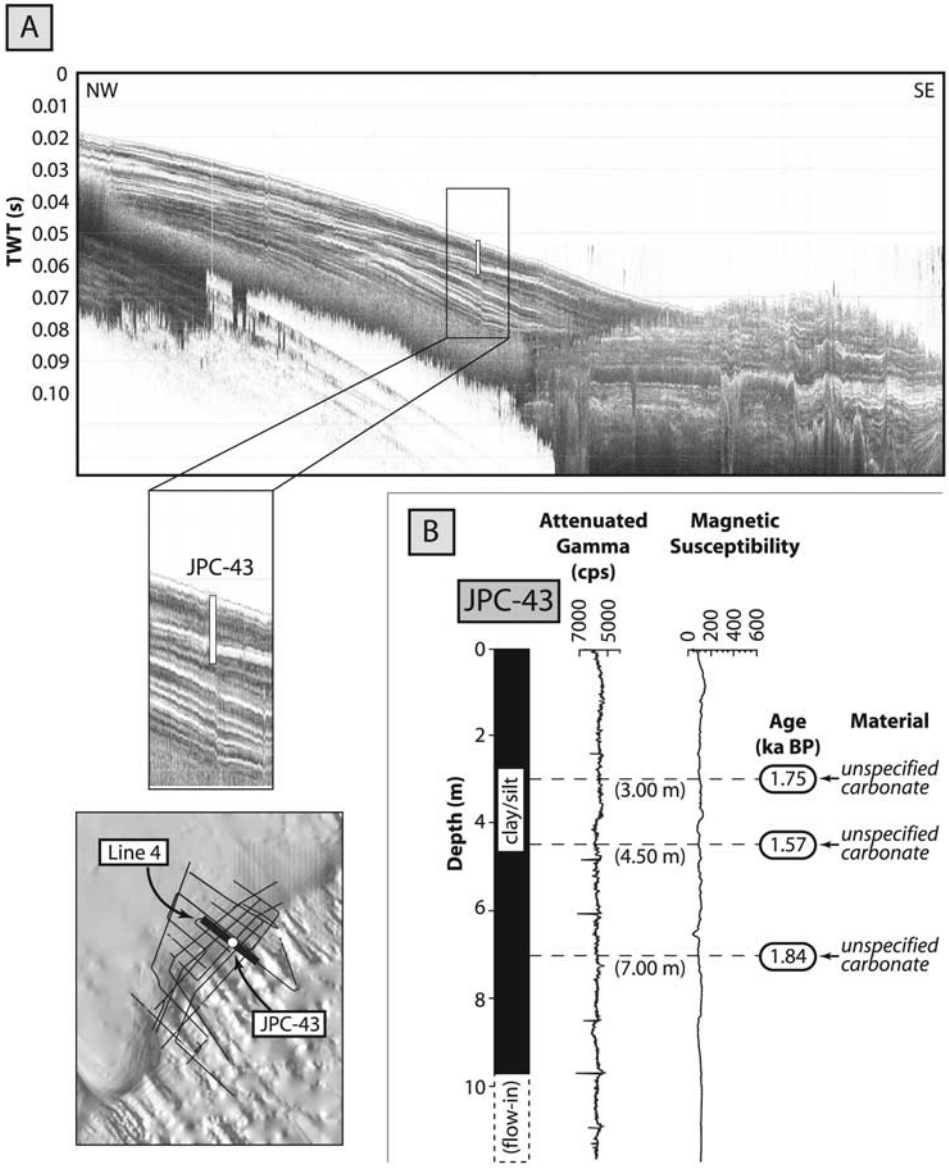

Figure 9. (a) Chirp dip line PNG4L10 near toe of modern clinothem showing location of JPC-43. (b) Core lithic log, attenuated gamma and magnetic susceptibility logs, and radiocarbon ages. Acoustically transparent, very fine silt/clay intervals intercalated with medium thick beds of more reflective very fine sands downlap onto older clinothem. Surface S_1 is the light gray horizon just beyond the bottom of the core.

sea level rise following the LGM exhibits a regional dip toward the northwest. If the transgressive surface had minimal relief when it was formed by wave base erosion, then a dip of this magnitude requires a differential tectonic subsidence rate of $\sim$1 mm a^{-1}. Finally, it is interesting to note that high accumulation rates on the slope between 60,000–100,000 years BP are succeeded by lower rates from $\sim$30,000–55,000 years BP [*Mallarino et al.*, 2004], consistent with an increase of accommodation on the shelf in response to a relative sea level rise produced by tectonic subsidence.

[27] In the central gulf midshelf region NE of the Fly River mouth, the older clinothem has been dissected by six major valleys and numerous channels (cf. Figure 4). We interpret this erosion to be fluvial in origin and to have occurred during the rapid eustatic fall commencing $\sim$25 ka BP (Stage 2) that lowered sea level to $-$125 m. An alternative hypothesis is that they are tidally incised shelf valleys in the manner of *Harris et al.* [2005], but we consider this unlikely given the dendritic nature of the valley systems and the deep channels observed within the valleys (Figure 4d). As eustatic sea level rose from $-$125 to +3 m between 20 and 7 ka BP, the former midshelf river channels within the river valley were partially filled by fluvial and estuarine facies [*Milliman et al.*, 2006]. The transgression was so rapid however, that the valleys themselves remained unfilled except for minimal input from eroding interfluves. Farther landward near the Fly River

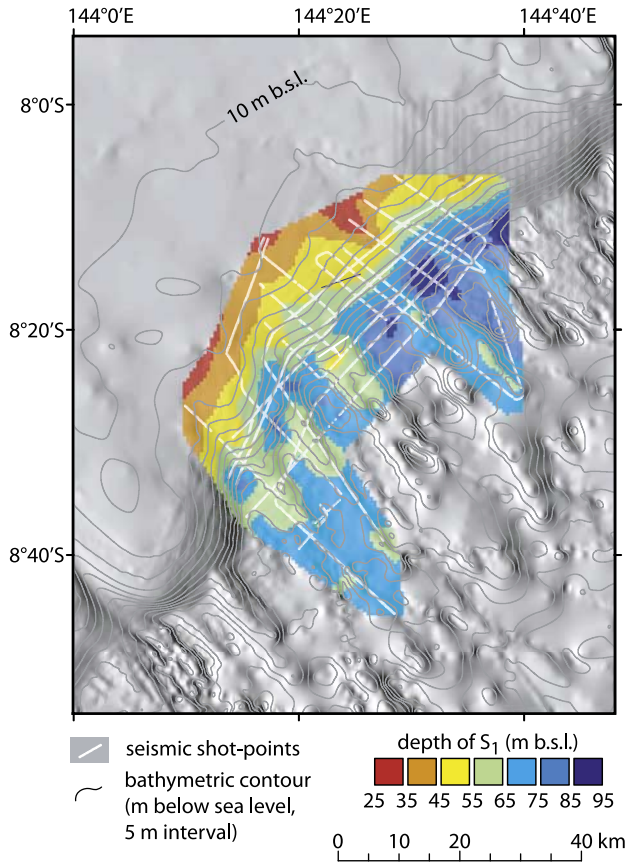

Figure 10. Shaded structure contour map of S_1 surface draped on modern smoothed bathymetric contours. See text for details.

mouth, more of the transgressive systems tract (TST) was preserved [*Harris et al.*, 1996], but even there it remains thin and discontinuous. In most places the sequence boundary, the transgressive surface, and the maximum flooding surface coalesce (e.g., Figure 4a). When and where a Holocene GoP clinothem began advancing seaward remains unknown; the turn around point lies landward of our data. The Holocene clinothem had prograded to within 15 km of its present position by about 4.8 ka BP, although the Yellow unit may be older than 9–9.5 ka BP (i.e., MWP 1C). This early growth produced acoustically high-amplitude reflectors that exhibit oblique progradation at the top of the Yellow unit (Figures 6 and 7), indicating that sediment supply was greater than the creation rate of new accommodation and filled all the available accommodation. Stratal strike profiles show undulations in the clinoform surface caused by the mesas and valleys over which the Holocene clinothem was prograding (Figure 12). The folds in the Yellow unit in the NE corner of the study area appear to record continued downslope soft sediment deformation during clinothem growth. The Orange and Red units downlap onto the S_1 surface and this requires the generation of new accommodation after the deposition of the Yellow unit. Given the uncertainty in the age of S_1, two possible scenarios might explain how the new accommodation was formed. In scenario 1, the oblique clinoforms of the Yellow unit were formed during a eustatic stillstand approximately 9–9.5 ka BP. A subsequent rapid rise in sea level during MWP 1C (dated in the Great Barrier Reef and in southern Asia at 9.1–9.6 ka BP [*Larcombe and Carter*, 1998; *Liu et al.*, 2004b]) produced the S_1 surface and the accommodation in which the finer-grained Orange and Red units came to downlap the Yellow unit (Figures 5 and 6). Alternatively, if the ^{14}C dates from the flow-in of core JPC-40 (Figure 8) come from both above and below S_1, then the age of S_1 lies between 2.41 and 5.2 ka BP. Because there are no known rapid rises of sea level during this interval, S_1 must be due to a rapid decline in the rate of sediment supply at a constant subsidence rate. In scenario 2, the oblique clinoforms are formed during a period of high sediment supply and then the sediment supply is shut off and long-term subsidence accounts for the generation of the new accommodation and formation of the downlap surface. We can find no evidence from other studies to decide between the two scenarios. Longer cores are required to test these two alternatives.

[28] Clinothem growth resumed after the S_1 event as localized sedimentation of the Orange unit in the southern half of the study area. It fills local accommodation, offlapping both to the north and south. By approximately 1.6 ka BP ago, sediments of the Red unit began to blanket the whole study area. These latest sediments consist of an acoustically transparent facies that forms an on- and downlapping toe of the wedge. The thickness of the Red unit

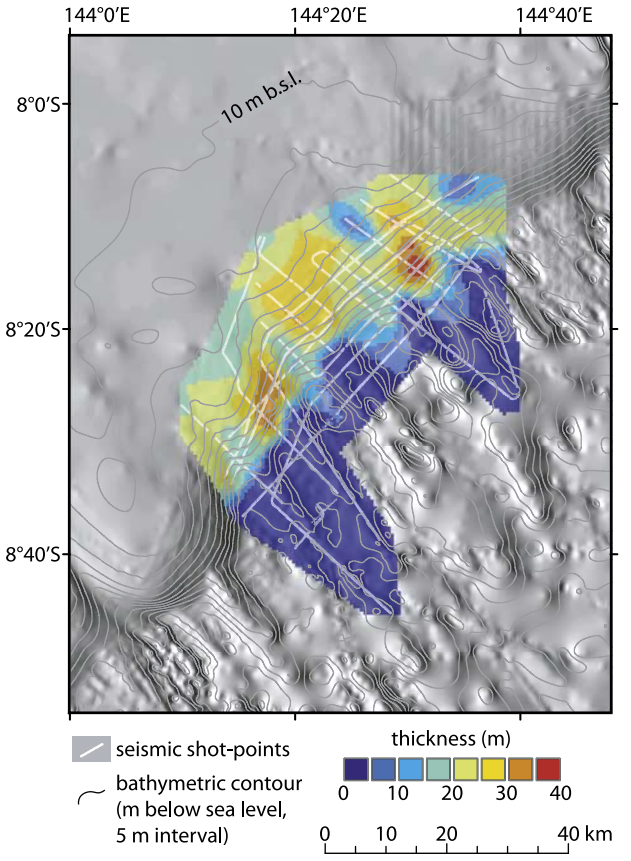

Figure 11. Isopach map of the interval between the S_1 surface and the seafloor, draped over shaded bathymetry. Note that on the upper clinoform face the Orange and Red units are thickest over promontories in underlying landscape, but at the clinoform toe they are thickest in reentrants. See text for details.

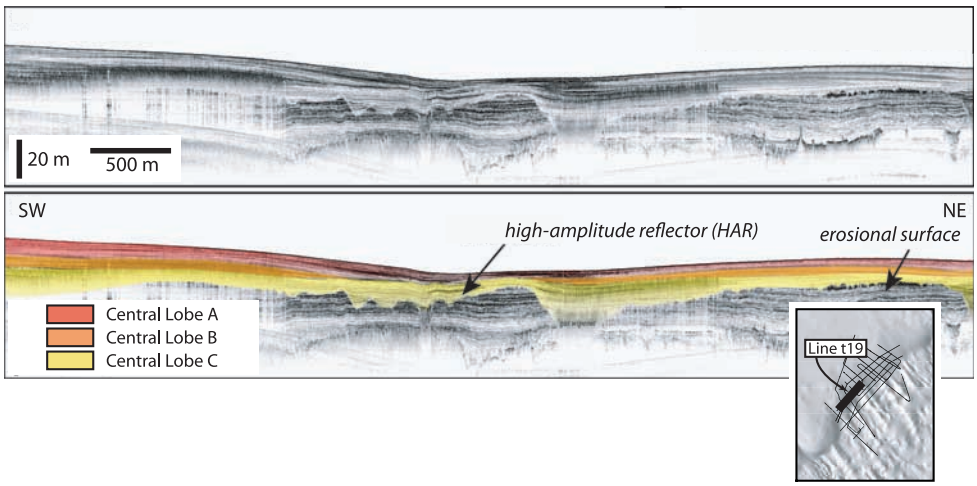

Figure 12. Chirp seismic profile across central lobe illustrating the differential thickness of the upper two units (Orange and Red) being thickest on the promontories and thinnest in the valleys. Note high-amplitude reflectors within the valleys that correlate with sands.

exhibits less variability than the Orange (Figures 6, 7, and 12). This transparent facies appears to be sediment winnowed from upslope strata, suggesting that at present, clinothem progradation may be moribund. The thickness variability observed in the isopachs as well as the high-amplitude reflectors observed in the valleys suggest that the dominant transport is strongly oblique to the isobaths and both northeast and southwest directed.

[29] Mineralogy of the uppermost beds of the Holocene clinothem also indicate significant bidirectional alongshore sediment transport (Figure 14). The Fly River sediment consists of mature illite clay and quartz-rich sands, consistent with its source rock composition and long distance of transport. Sediments of the northern rivers such as the Kikori and Purari consist of immature smectite clays and lithic sands with a strong volcanic component. Sediments of the modern shelf represent a mixture of these two types. This mixed assemblage can only be explained by at least some component of southerly transport along much of the upper tread with a convergence zone just north of the Fly River where sediment is shunted seaward off the shelf.

5.2. Modes of Clinothem Growth

[30] The Holocene GoP clinothem has not formed by simple parallel progradation of topsets over irregular bathymetry. Rather, the clinothem is composed of discrete lobes that formed at separate times. Cross-cutting relationships among the shingled lobes indicate that overall development of the clinothem complex has progressed from the center of the study area outward. These lobes are the fundamental architectural elements of the modern clinothem's stratigraphy. They consist of both onlapping and downlapping reflectors, suggesting that depocenters originated and accreted on the clinothem face, expanding updip and downdip as well as laterally. The pattern of paired onlapping and downlapping is particularly evident in the thickest (central and southwestern) parts of each clinothem segment. This architecture requires a sediment transport process such as sedimentation from suspension or failed

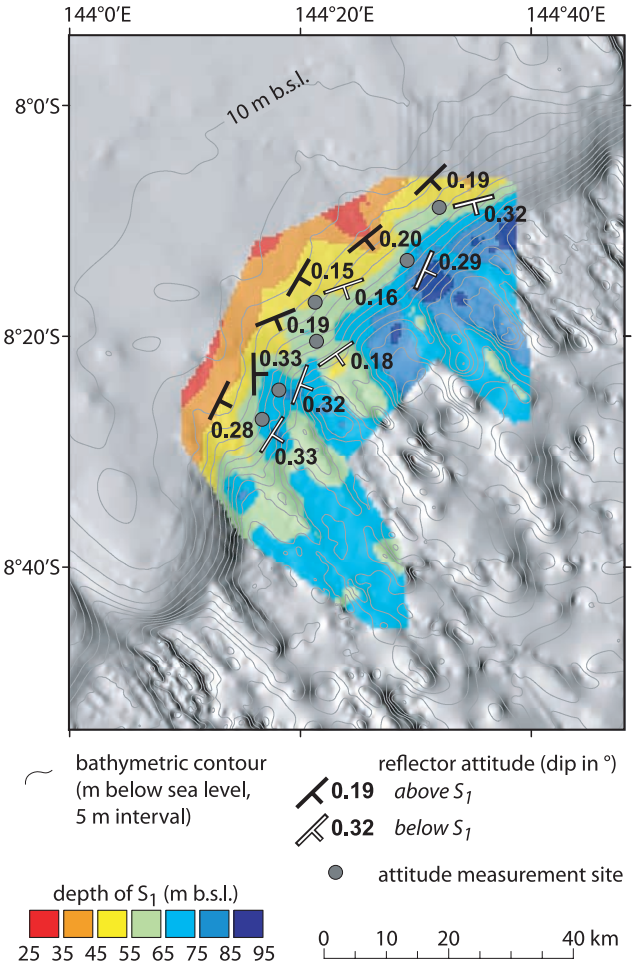

Figure 13. Reflector dips of strata above and below S_1, showing that dip directions are roughly similar indicating self-similar progradation.

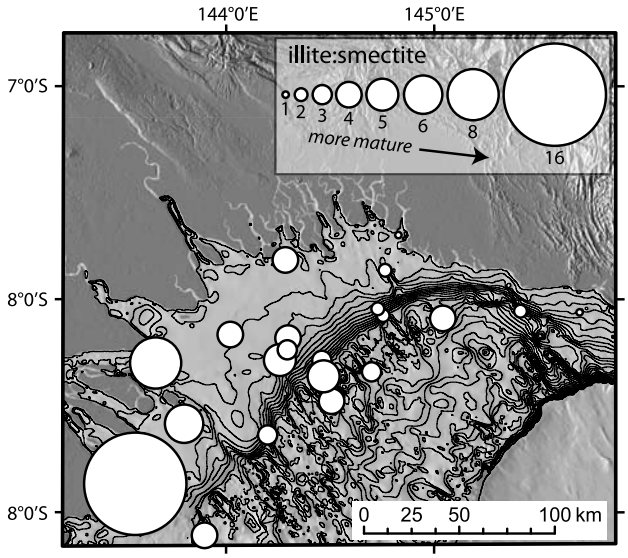

Figure 14. Illite/smectite ratios of the clay size fraction in surface sediments of the Gulf of Papua. Ratio increases systematically from northeast to southwest, indicating smectite-dominated rivers to the northeast contribute a large fraction relative to the illite-dominated Fly River to southwest.

gravity flows that produces initial vertical accretion on the clinoform face and then extension of the locus of deposition both upslope and downslope. The volume of sediment per unit distance along strike deposited since S_1 time can be estimated from the isopach map (Figure 11) to be 420,000 m^2. For a mean vertical thickness above S_1 of 16.2 m and a mean modern clinoform slope of 0.14°, the mean distance of recent clinoform progradation equals 6.6 km, and the mean clinothem vertical sedimentation rate is between 1 and 5 mm a^{-1}. Because the analysis area does not extend completely to the updip end of the clinothem, these values should be considered minimal. This vertical sedimentation rate is smaller by an order of magnitude than short-term sedimentation rates of 1–4 cm a^{-1} reported by *Harris et al.* [1996] and *Walsh et al.* [2004], based on ^{210}Pb and short-core ^{14}C dates, but are consistent with rates of 3 to 4 mm a^{-1} computed using about twenty AMS ^{14}C dates from our cores, which range from a few hundred years to a few thousand years old (see the Marine Geoscience Data System at http://www.marine-geo.org/link/entry.php?id) = VANC23MV for core descriptions and locations). Although it is well known that sedimentation rates calculated using dates spanning greater stratigraphic intervals are always lower [*Gardner et al.*, 1987], this effect cannot explain the magnitude of the discrepancy here over such a relatively young time range of hundreds to a few thousands of years.

[31] Our data indicate that during the formation of the Holocene clinothem, the northern rivers in the Gulf of Papua were supplying much sediment to the midshelf region and filling the available accommodation. Near the Fly River in the southern gulf, sediment input to the region was less than the available accommodation, resulting in the formation of sigmoidal clinoforms.

[32] Can changes in sediment transport patterns explain the S_1 and S_2 surfaces and the shifting loci of deposition? Computed annual circulation of the GoP in response to

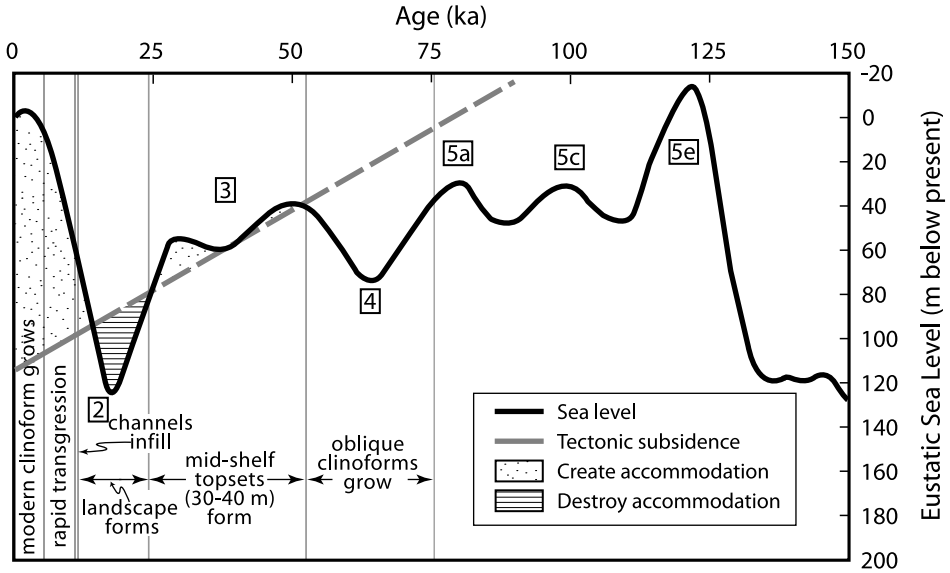

Figure 15. Inferred formation of the Gulf of Papua clinothems. Older, partially eroded clinothem consists of approximately 30–40 m of generally subparallel reflectors mantling a set of obliquely prograding reflectors. Deflection of the transgressive surface from horizontal yields a post-LGM differential subsidence of about 1 mm a^{-1} from the peripheral bulge in the southwest to near the basin depocenter in the northeast. On the basis of the *Lambeck and Chappell* [2001] and *Chappell and Shackleton* [1986] eustatic sea level curve, eustatic sea level fell from ~−40 to ~−65 m between 45 and 25 ka BP. Older clinothem topsets are thought to have accumulated at the end of Stage 3 about 30 ka BP as accommodation space was created by a relative slowing of sea level fall.

trade wind and monsoon conditions shows that the flow fields are significantly different [*Slingerland et al.*, 2008]. Possibly the surfaces and lobes were created by century to millennial-scale changes in the wind fields. This can be a sufficient explanation only if the change in circulation changed the amount of accommodation, because that is the only way to explain oblique offlap changing to aggradation. The most obvious way to do this is to change wave base significantly.

6. Conclusions

[33] The upper 100 m of the Gulf of Papua shelf are composed of two stacked clinothems: an older deeply eroded clinothem forming the middle and outer shelf, and a superjacent younger clinothem extending from the coast offshore forming the inner shelf. The older, partially eroded clinothem was built during Stages 4 and 3, eroded into a series of northwest-southeast trending paleovalleys and mesas during Stage 2, and partially covered by a younger clinothem during Stage 1. The younger clinothem downlaps onto the erosional surface etched into topsets of the older clinothem. It consists of three major stratigraphic units that are separated by two surfaces of erosion or bypass or correlative surfaces of down/up/on/off-lap. The ages and origins of these surfaces are not well known, however the formation of S_1 and its mantle of downlapping strata requires the formation of new accommodation. This stratal geometry cannot be formed by simple lobe switching. We present two scenarios to explain the formation of the new accommodation: changes in the rate of eustatic sea level rise, or changes in the rate of sediment supply with long-term tectonic subsidence.

[34] Isopach patterns, mapped terminations on the regional unconformity, and seismic patterns in the central study area indicate an early phase of clinothem growth below S_1 occurred by oblique progradation of acoustically high-amplitude, well-bedded reflectors on the clinoform face. This phase was succeeded by aggrading onlapping and downlapping acoustically transparent units (Orange and Red). These lithosomes tend to be elongate in the downdip direction and form generally on modern bathymetric promontories. Since formation of S_1, the clinothem has grown vertically by an average of 16 m and advanced shelfward an average distance of 6 km, yielding a mean clinothem vertical sedimentation rate of about 1 to 5 mm a^{-1}. The rates are variable along the present clinoform face. Sediment transport is predominantly off-shelf with the fine-grained material deposited on the highs with bypass and off-shelf transport in the valleys. Off-shelf transport must be oblique across the clinoform face, both NE and SW directed, to account for the directions of lap.

[35] Our study highlights the importance of the underlying physiography in controlling sediment dispersal and accumulation on the Gulf of Papua margin and shows that the Holocene clinothem there is inherently three-dimensional, consisting of lobes within lobes. The observed and computed modern flows and complex gyres in shallow water coupled with wave- and current-supported gravity flows or river floods can explain the form, internal clinoform shapes, and mineralogy of the younger Gulf of Papua clinothem. This knowledge provides a first step toward developing a quantitative understanding of its formation, but the origins of the changes in accommodation remain unknown.

[36] **Acknowledgments.** This research was supported by National Science Foundation awards 0305699, 0305779, and 0305607 under the MARGINS Initiative. Special thanks to the crew of the R/V *Melville*, the Oregon State University Coring Facility, and J. Hill, R. Fenwick, and J. Walsh who participated on the cruise.

References

Aller, R. C., N. E. Blair, and G. J. Brunskill (2008), Early diagenetic cycling, incineration, and burial of sedimentary organic carbon in the central Gulf of Papua (Papua New Guinea), *J. Geophys. Res.*, *113*, F01609, doi:10.1029/2006JF000689.

Bartek, L. R., P. R. Vail, J. B. Anderson, P. A. Emmet, and S. Wu (1991), Effect of Cenozoic ice sheet fluctuations in Antarctica on the stratigraphic signature of the Neogene, *J. Geophys. Res.*, *96*, 6753–6778.

Berne, S., M. Rabineau, J. A. Flores, and F. J. Sierro (2004), The impact of Quaternary global changes on strata formation, *Oceanography*, *17*(4), 92–103.

Brunskill, G. J. (2004), New Guinea and its coastal seas, a testable model of wet tropical coastal processes: an introduction to Project TROPICS, *Cont. Shelf Res.*, *24*(19), 2273–2295.

Cattaneo, A., F. Trincardi, L. Langone, A. Asioli, and P. Puig (2004), Clinoform generation on Mediterranean margins, *Oceanography*, *17*(4), 105–117.

Chappell, J., and N. J. Shackleton (1986), Oxygen isotopes and sea level, *Nature*, *324*(6093), 137–140.

Chen, Z., Y. Saito, K. Hori, Y. Zhao, and A. Kitamura (2003), Early Holocene mud-ridge formation in the Yangtze offshore, China: A tidal-controlled estuarine pattern and sea-level implications, *Mar. Geol.*, *198*(3–4), 245–257.

Christie-Blick, N., and N. W. Driscoll (1995), Sequence stratigraphy, *Annu. Rev. Earth Planet. Sci.*, *23*, 451–478.

Daniell, J. J. (2008), Development of a bathymetric grid for the Gulf of Papua and adjacent areas: A note describing its development, *J. Geophys. Res.*, doi:10.1029/2006JF000673, in press.

Davies, P. J., P. A. Symonds, D. A. Feary, and C. J. Pigram (1989), The evolution of the carbonate platforms of northeast Australia, *Spec. Publ. Soc. Econ. Paleontol. Mineral.*, *44*, 233–258.

Deibert, J. E., T. Benda, T. Loseth, M. Schellpeper, and R. J. Steel (2003), Eocene clinoform growth in front of a storm-wave-dominated shelf, Central Basin, Spitsbergen: No significant sand delivery to deepwater areas, *J. Sediment. Res.*, *73*(4), 546–558.

Driscoll, N. W., and G. D. Karner (1999), Three-dimensional quantitative modeling of clinoform development, *Mar. Geol.*, *154*(1–4), 383–398.

Droxler, A., G. Mallarino, J. M. Francis, J. Dickens, B. N. Opdyke, L. Beaufort, J. Daniell, S. J. Bentley, and L. C. Peterson (2006), Early transgressive establishment of relict upper most Pleistocene barrier reefs on LGM coastal siliciclastic deposits in the Gulf of Papua and Gulf of Mexico: Clue to understand the mid Brunhes global origin of modern barrier reefs, paper presented at Catchments to the Coast, Australian Marine Sciences Association 44th Annual Conference, Soc. of Wetland Scientists, Cairns, Queensland, Australia, 9–14 July.

Gardner, T. W., D. W. Jorgensen, C. Shuman, and C. R. Lemieux (1987), Geomorphic and tectonic process rates: Effects of measured time interval, *Geology*, *15*(3), 259–261.

Hampson, G. J., and J. E. A. Storms (2003), Geomorphological and sequence stratigraphic variability in wave-dominated, shoreface-shelf parasequences, *Sedimentology*, *50*(4), 667–701.

Harris, P. T. (1990), Sedimentation at the junction of the Fly River and the northern Great Barrier Reef, in *Torres Strait Baseline Study Conference*, edited by D. Lawrence and T. Cansfield-Smith, pp. 59–85, Queensland, Australia.

Harris, P. T., C. B. Pattiaratchi, J. B. Keene, R. W. Dalrymple, J. W. Gardner, E. K. Baker, A. R. Cole, D. M. Mitchell, P. Gibbs, and W. W. Schroeder (1996), Late Quaternary deltaic and carbonate sedimentation in the Gulf of Papua foreland basin: Response to sea-level change, *J. Sediment. Res.*, *66*(4), 801–819.

Harris, P. T., M. G. Hughes, E. K. Baker, R. W. Dalrymple, and J. B. Keene (2004), Sediment transport in distributary channels and its export to the pro-deltaic environment in a tidally dominated delta: Fly River, Papua New Guinea, *Cont. Shelf Res.*, *24*(19), 2431–2454.

Harris, P. T., A. Heap, V. Passlow, M. Hughes, J. Daniell, M. Hemer, and O. Anderson (2005), Tidally incised valleys on tropical carbonate

shelves: An example from the northern Great Barrier Reef, Australia, *Mar. Geol.*, *220*, 181–204.
Hemer, M. A., P. T. Harris, R. Coleman, and J. Hunter (2004), Sediment mobility due to currents and waves in the Torres Strait-Gulf of Papua region, *Cont. Shelf Res.*, *24*(19), 2297–2316.
Hori, K., Y. Saito, Q. Zhao, and P. Wang (2002b), Evolution of the coastal depositional systems of the Changjiang (Yangtze) river in response to late Pleistocene-Holocene sea-level changes, *J. Sediment. Res.*, *72*(6), 884–897.
Keen, T. R., D. S. Ko, R. L. Slingerland, S. Riedlinger, and P. Flynn (2006), Potential transport pathways of terrigenous material in the Gulf of Papua, *Geophys. Res. Lett.*, *33*, L04608, doi:10.1029/2005GL025416.
Kineke, G. C., R. W. Sternberg, J. H. Trowbridge, and W. R. Geyer (1996), Fluid-mud processes on the Amazon continental shelf, *Cont. Shelf Res.*, *16*(5–6), 667–696.
Kostic, S., and G. Parker (2003a), Progradational sand-mud deltas in lake and reservoirs. part 1: Theory and numerical modeling, *J. Hydraul. Res.*, *41*(2), 127–140.
Kostic, S., and G. Parker (2003b), Progradational sand-mud deltas in lakes and reservoirs. part 2: Experimental and numerical simulation, *J. Hydraul. Res.*, *41*(2), 141–152.
Kuehl, S. A., D. J. DeMaster, and C. A. Nittrouer (1986), Nature of sediment accumulation on the Amazon continental shelf, *Cont. Shelf Res.*, *6*(1–2), 209–225.
Kuehl, S. A., T. M. Hariu, and W. S. Moore (1989), Shelf sedimentation off the Ganges-Brahmaputra river system; evidence for sediment bypassing to the Bengal Fan, *Geology*, *17*(12), 1132–1135.
Kuehl, S. A., C. A. Nittrouer, M. A. Allison, L. Ercilio, C. Faria, D. A. Dukat, J. M. Jaeger, T. D. Pacioni, A. G. Figueiredo, and E. C. Underkoffler (1996), Sediment deposition, accumulation, and seabed dynamics in an energetic fine-grained coastal environment, *Cont. Shelf Res.*, *16*(5–6), 787–815.
Kuehl, S. A., M. A. Allison, S. L. Goodbred, and H. Kudrass (2005), The Ganges-Brahmaputra Delta, in *River Deltas: Concepts, Models, and Examples*, edited by L. Gosian and J. Bhattacharya, *Spec. Publ. Soc. Econ. Paleontol. Mineral.*, *83*, 413–434.
Lambeck, K., and J. Chappell (2001), Sea level change through the last glacial cycle, *Science*, *292*(5517), 679–686.
Larcombe, P., and R. M. Carter (1998), Sequence architecture during the Holocene transgression: An example from the Great Barrier Reef shelf, Australia, *Sediment. Geol.*, *117*(1–2), 97–121.
Liu, J. P., A. C. Li, Z. S. Yang, K. H. Xu, and J. D. Milliman (2004a), Sediment flux and fate of the Yangtze River sediments delivered to the East China Sea, *Eos Trans. AGU*, *85*(47), Fall Meet. Suppl., Abstract OS23C-1319.
Liu, J. P., J. D. Milliman, S. Gao, and P. Cheng (2004b), Holocene development of the Yellow River's subaqueous delta, north Yellow Sea, *Mar. Geol.*, *209*, 45–67.
Lofi, J., et al. (2003), Plio-Quaternary prograding clinoform wedges of the western Gulf of Lion continental margin (NW Mediterranean) after the Messinian salinity crisis, *Mar. Geol.*, *198*(3–4), 289–317.
Mallarino, G., J. M. Francis, A. W. Droxler, B. N. Opdyke, S. J. Bentley, G. R. Dickens, and L. C. Peterson (2004), Uppermost Pleistocene sea-level transgression across a Last Glacial Maximum mixed carbonate/siliciclastic coastline, modern Gulf of Papua shelf break in the northern Ashmore Trough, *Eos Trans. AGU*, *85*(47), Fall Meet. Suppl., Abstract OS51B-1303.
McCormick, D. S., J. B. Thurmond, J. P. Grotzinger, and R. J. Fleming (2000), Creating a three-dimensional model of clinoforms in the upper San Andres Formation, Last Chance Canyon, New Mexico, paper presented at AAPG Annual Meeting, Am. Assoc. of Pet. Geol., New Orleans, Louisiana, 16–19 April.
Michels, K. H., H. R. Kudrass, C. Huebscher, A. Suckow, and M. Wiedicke (1998), The submarine delta of the Ganges-Brahmaputra: Cyclone-dominated sedimentation patterns, *Mar. Geol.*, *149*(1–4), 133–154.
Milliman, J. D. (1995), Sediment discharge to the ocean from small mountainous rivers: The New Guinea example, *Geo Mar. Lett.*, *15*(3–4), 127–133.
Milliman, J. D., K. L. Farnsworth, and C. S. Albertin (1999), Flux and fate of fluvial sediments leaving large islands in the East Indies, *J. Sea Res.*, *41*, 97–107.
Milliman, J. D., K. Xu, G. J. Brunskill, R. Slingerland, and N. W. Driscoll (2006), Sediment mineralogy on the Gulf of Papua clinoform: New insights into sediment sources and redistribution processes, *Eos Trans. AGU*, *87*(36), Ocean Sci. Meet. Suppl., Abstract OS16A-25.
Mitchum, R. M., Jr., P. R. Vail, and J. B. Sangree (1977), Seismic stratigraphy and global changes of sea level. part 6: Stratigraphic interpretation of seismic reflection patterns in depositional sequences, in *Seismic Stratigraphy: Applications to Hydrocarbon Exploration*, edited by C. E. Payton, pp. 135–143, *Am. Assoc. of Petrol. Geol.*, Tulsa, Okla.
Moore, R., and W. MacFarlane (1984), Migration of ornate rock lobster, *Panulirus ornatus* (Fabricius), in Papua New Guinea, *Aust. J. Mar. Freshwater Res.*, *35*, 197–212.
Niedoroda, A. W., C. W. Reed, H. Das, S. Fagherazzi, J. F. Donoghue, and A. Cattaneo (2005), Analyses of a large-scale depositional clinoformal wedge along the Italian Adriatic coast, *Mar. Geol.*, *222/223*, 179–192.
Nittrouer, C. A., and D. J. DeMaster (1996), The Amazon shelf setting: Tropical, energetic, and influenced by a large river, *Cont. Shelf Res.*, *16*(5–6), 553–573.
Nittrouer, C. A., S. A. Kuehl, D. J. DeMaster, and R. O. Kowsmann (1986), The deltaic nature of Amazon shelf sedimentation, *Geol. Soc. Am. Bull.*, *97*(4), 444–458.
Nittrouer, C. A., S. A. Kuehl, R. W. Sternberg, A. G. Figueiredo Jr., and L. E. C. Faria (1995), An introduction to the geological significance of sediment transport and accumulation on the Amazon continental shelf, *Mar. Geol.*, *125*(3–4), 177–192.
Nittrouer, C. A., S. A. Kuehl, A. G. Figueiredo, M. A. Allison, C. K. Sommerfield, J. M. Rine, L. E. C. Faria, and O. M. Silveira (1996), The geological record preserved by Amazon shelf sedimentation, *Cont. Shelf Res.*, *16*(5–6), 817–841.
Ogston, A. S., J. S. Crockett, R. W. Sternberg, and C. A. Nittrouer (2003), Sediment transport under monsoon conditions on the Fly River clinoform, Papua New Guinea, *Eos. Trans. AGU*, *84*, Fall Meet. Suppl., Abstract OS11A-05.
Ogston, A. S., R. W. Sternberg, C. A. Nittrouer, D. P. Martin, M. A. Goñi, and J. S. Crockett (2004), Factors leading to the spatial heterogeneity of sediment-transport processes on the Fly River clinoform, Gulf of Papua, *Eos Trans. AGU*, *85*(47), Fall Meet. Suppl., Abstract OS44A-03.
Ogston, A. S., J. S. Crockett, M. A. Goni, C. A. Nittrouer, D. P. Martin, and R. W. Sternberg (2008), Sediment delivery from the Fly River tidally dominated delta to the nearshore marine environment and the impact of El Niño, *J. Geophys. Res.*, *113*, F01S11, doi:10.1029/2006JF000669.
Olariu, C., and J. P. Bhattacharya (2006), Terminal distributary channels and delta front architecture of river-dominated delta systems, *J. Sediment. Res.*, *76*(2), 212–233.
Paola, C., et al. (2001), Experimental stratigraphy, *GSA Today*, *11*(7), 4–9.
Pickup, G. (1984), Geomorphology of tropical rivers: I. Landforms, hydrology and sedimentation in the Fly and Lower Purari, Papua New Guinea, *Catena Suppl.*, *5*, 1–17.
Pirmez, C., L. F. Pratson, and M. S. Steckler (1998), Clinoform development by advection-diffusion of suspended sediment: Modeling and comparison to natural systems, *J. Geophys. Res.*, *103*(B10), 24,141–24,157.
Poulsen, C. J., P. B. Flemings, R. A. J. Robinson, and J. M. Metzger (1998), Three-dimensional stratigraphic evolution of the Miocene Baltimore Canyon region: Implications for eustatic interpretations and the systems tract model, *Geol. Soc. Am. Bull.*, *110*(9), 1105–1122.
Pratson, L. F., et al. (2004), Modeling continental shelf formation in the Adriatic Sea and elsewhere, *Oceanography*, *17*(4), 119–131.
Salomons, W., and A. M. Eagle (1990), Hydrology, sedimentology and the fate and distribution of copper in mine-related discharges in the Fly River system, Papua New Guinea, *Sci. Total Environ.*, *97/98*, 315–334.
Slingerland, R., R. W. Selover, A. S. Ogston, T. R. Keen, N. W. Driscoll, and J. D. Milliman (2008), Building the Holocene clinothem in the Gulf of Papua: An ocean circulation study, *J. Geophys. Res.*, doi:10.1029/2006JF000680, in press.
Steckler, M. S., G. S. Mountain, K. G. Miller, and N. Christie-Blick (1999), Reconstruction of Tertiary progradation and clinoform development on the New Jersey passive margin by 2-D backstripping, *Mar. Geol.*, *154*(1–4), 399–420.
Walsh, J. P., C. A. Nittrouer, C. M. Palinkas, A. S. Ogston, R. W. Sternberg, and G. J. Brunskill (2004), Clinoform mechanics in the Gulf of Papua, New Guinea, *Cont. Shelf Res.*, *24*(19), 2487–2510.
Wolanski, E., and D. M. Alongi (1995), A hypothesis for the formation of a mud bank in the Gulf of Papua, *Geo Mar. Lett.*, *15*(3–4), 166–171.
Wolanski, E., G. L. Pickard, and D. L. B. Jupp (1984), River plumes, coral reefs and mixing in the Gulf of Papua and the northern Great Barrier Reef, *Estuarine Coastal Shelf Sci.*, *18*(3), 291–314.
Wolanski, E., A. Norro, and B. King (1995), Water circulation in the Gulf of Papua, *Cont. Shelf Res.*, *15*, 185–212.

N. W. Driscoll and E. A. Johnstone, Scripps Institution of Oceanography, GRD 0244, La Jolla, CA 92093, USA.
S. R. Miller and R. Slingerland, Department of Geosciences, 513A Deike, Pennsylvania State University, University Park, PA 16802, USA.
J. D. Milliman, School of Marine Science, College of William and Mary, 1208 Greate Road, Gloucester Point, VA 23062, USA.